




Adjustable magnetic and wear properties of gradient Al–stainless steel materials fabricated by direct energy deposition

O. N. Dubinin^{1,4} · D. A. Chernodubov² · A. S. Semenyuk^{3,4} · D. G. Shaysultanov³ · S. V. Zhrebtsov^{3,4} · S. A. Evlashin¹ · N. D. Stepanov^{3,4} 

Received: 18 August 2023 / Accepted: 9 September 2024 / Published online: 16 September 2024
© The Author(s), under exclusive licence to Springer Nature Switzerland AG 2024

Abstract

Additive manufacturing enables the efficient production of intricate parts and the creation of multi-material mixtures of functionally graded materials. Such materials can demonstrate spatially variable mechanical and functional properties and thus can be attractive for various applications. In this work, we have produced gradient materials from a mixture of 316L stainless steel and pure Al by direct energy deposition. It was revealed that a relatively small (5–10 wt.%) addition of Al can turn paramagnetic steel into the ferromagnetic material with saturation magnetization up to 118 emu g^{−1} and enhance the wear resistance from $\sim 6 \times 10^{-4}$ to $\sim 1.5 - 3.0 \times 10^{-5}$ mm²/N/m. The changes in properties were associated with the transformation of the FCC structure of steel to dual-phase BCC + B2, which occurred in reasonable agreement with the CALPHAD calculations. The obtained gradient materials can be possibly used for cost-effective shielding applications.

Keywords Direct energy deposition · Gradient materials · Phase transformations · Magnetic properties · Wear resistance

1 Introduction

Additive manufacturing (AM) is a group of methods for manufacturing of complex-shaped products using the existing 3D models through layer-by-layer deposition of selected material(s) [1]. AM can offer considerable improvements in productivity and cost-efficiency over traditional processes in a variety of applications. Metallic AM typically employs laser or electron beams to deposit the materials in a form of powders or wires [2]. It is already widely applied in various industries, from aerospace to medicine [3, 4].

However, current metallic AM technologies largely focus on load-bearing applications. Meanwhile, there is a

significant interest in other fields, such as magnetic applications [5]. Fabrication of complex-shaped parts from magnetic alloys using traditional approaches is cost- and time-consuming [6]. Unlike the mechanical properties [7, 8], magnetic properties of the AM materials can tend to deteriorate. For example, soft magnetic materials such as Fe–Ni or Fe–Co alloys produced using AM tend to exhibit inferior magnetic properties to their conventional counterparts [9, 10].

Another interesting opportunity provided by AM technologies is associated with the formation of the gradient materials [11, 12]. AM techniques like direct energy deposition (DED) allow a wide range chemical composition variation in produced parts thus enabling the adjustment of the structure and properties [13]. One of the best-known examples of gradient materials are related to mechanical properties [14, 15]. However, there are also some examples of gradient magnetic materials, such as high entropy alloys of Fe–Ni/Fe–Co soft magnets [16, 17]. Moreover, the capacity to produce gradient magnetic materials from non-magnetic powders, i.e., 316L steel and Al–bronze (Cu–12Al–2Fe (in wt.%)), was recently demonstrated [18]. In addition, it is interesting to create multifunctional material with a set of tunable properties, i.e., magnetic and mechanical properties variable at the

✉ N. D. Stepanov
stepanov@bsu.edu.ru

¹ Center for Materials Technology, Skolkovo Institute of Science and Technology, 30, Bld. 1 Bolshoy Boulevard, Moscow 121205, Russia

² National Research Center “Kurchatov Institute”, P. I. Kurchatova, 1, Moscow 123182, Russia

³ Laboratory of Bulk Nanostructured Materials, Belgorod State University, Belgorod 308015, Russia

⁴ Saint-Petersburg State Marine Technical University, Lotsmanskaya Street, 3, Saint-Petersburg 190121, Russia

same time. For instance, wear can be a serious issue for such applications as electric motors [19]

To this end, in this letter, we demonstrate the capacity to simultaneously alter magnetic behavior and wear resistance in a gradient material made of widely used commercial 316L steel and pure Al.

2 Experimental procedures

Printing was performed using direct energy deposition (DED) technology on an Insteel MX-1000 machine. A mixture of metal powders of 316L stainless steel and pure aluminum in a given proportion was prepared in advance and loaded into the first feeder of the printer. The second feeder was loaded by 316L (Fig. 1). Round stainless steel 316L substrate with a diameter of 40 mm used for deposition of 20×20 mm and a thickness of 1 mm. The powder feed rate was calibrated using the built-in balance at 3.5 g/min. A g-code file was also prepared with a program for printing a cubic sample $10 \times 10 \times 10$ mm³ in size. G-code is a

language used to control CNC (computer numerical control) machines. It instructs the machine on how to move, what speed to use, and other parameters necessary for manufacturing parts or objects. The trajectory of the nozzle movement was a zig-zag, with a 90-degree turn on each layer. The distance between tracks was set at 500 μ m. The speed of print head movement was 850 mm/min, the layer height along the Z axis was 250 μ m, and a laser power was 380 W. After each layer, a pause of 5 s was applied for cooling of the printed layer. This set of printing parameters has been previously tested on 316L powder and showed very good results with low porosity and high geometrical accuracy. Samples with Al content ≤ 10 mass.% were selected for the study because of the strong cracking after reaching Al content of 10 mass.%.

The structure of the obtained samples was characterized by the scanning electron microscopy (SEM, FEI Quanta 600 FEG), electron-backscattered diffraction (EBSD, FEI Nova NanoSEM with EDAX Hikari detector) analysis, transmission electron microscopy (TEM, JEOL JEM-2100), and X-ray diffraction (XRD, Rigaku Ultima IV) analysis. Microstructure analysis was performed in the direction perpendicular to the build direction. Slabs with a mass of about 0.1 g were cut by electric discharge machine and used for magnetic properties measurements. The magnetic properties have been measured at 300 K with a Quantum Design PPMS vibrating sample magnetometer (VSM Option) in a range of fields from -2 T to 2 T.

Tribological characterization was performed at room temperature conditions using an Anton Paar high-temperature tribometer. A ceramic Al_2O_3 ball with a diameter of 6 mm was used as the counterbody. The friction coefficient was measured under a load of 2 N, at a movement speed of 5 cm/s, with a friction radius of 6 mm and a total length of 1000 m. The material wear was subsequently measured using a Nainovea PB 1000-point profilometer, and the wear parameters of the material were determined. Microhardness was measured using a Metatest ITV-1-AM instrument. The load during the measurement was 3 N, and measurements were taken at five points, with the data subsequently averaged.

The equilibrium phase diagrams were constructed using CALPHAD approach (ThermoCalc 2022a software, TCFE7.0 and TCHEA4 databases).

3 Results and discussion

The addition of Al had a significant impact on the magnetic properties of 316L steel. The measured magnetization curves are shown in Fig. 2a. The “pure” 316L steel did not exhibit ferromagnetic properties, however, the addition of Al resulted in ferromagnetic behavior of the steel. The

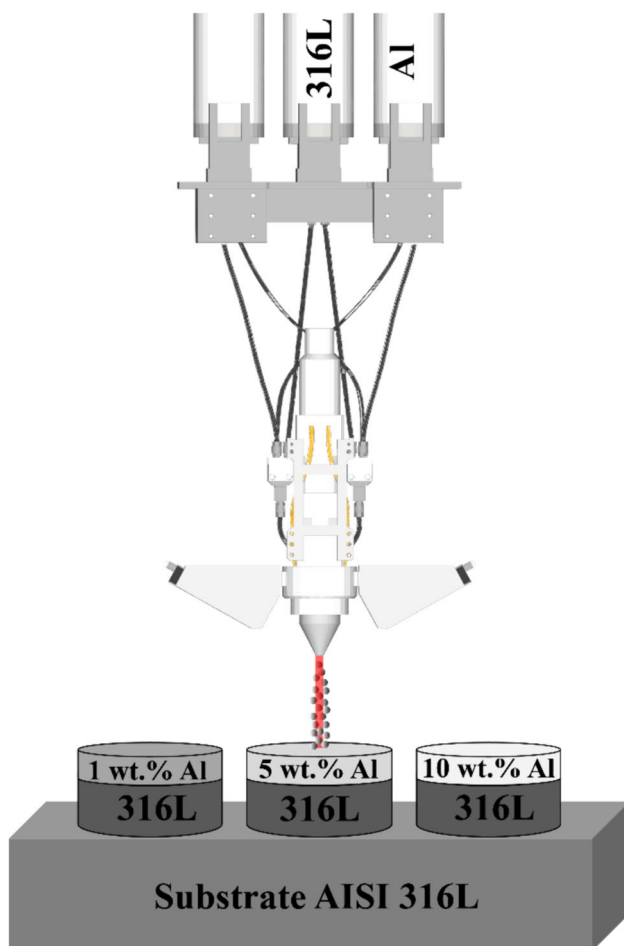


Fig. 1 The scheme of the DED of the program specimens

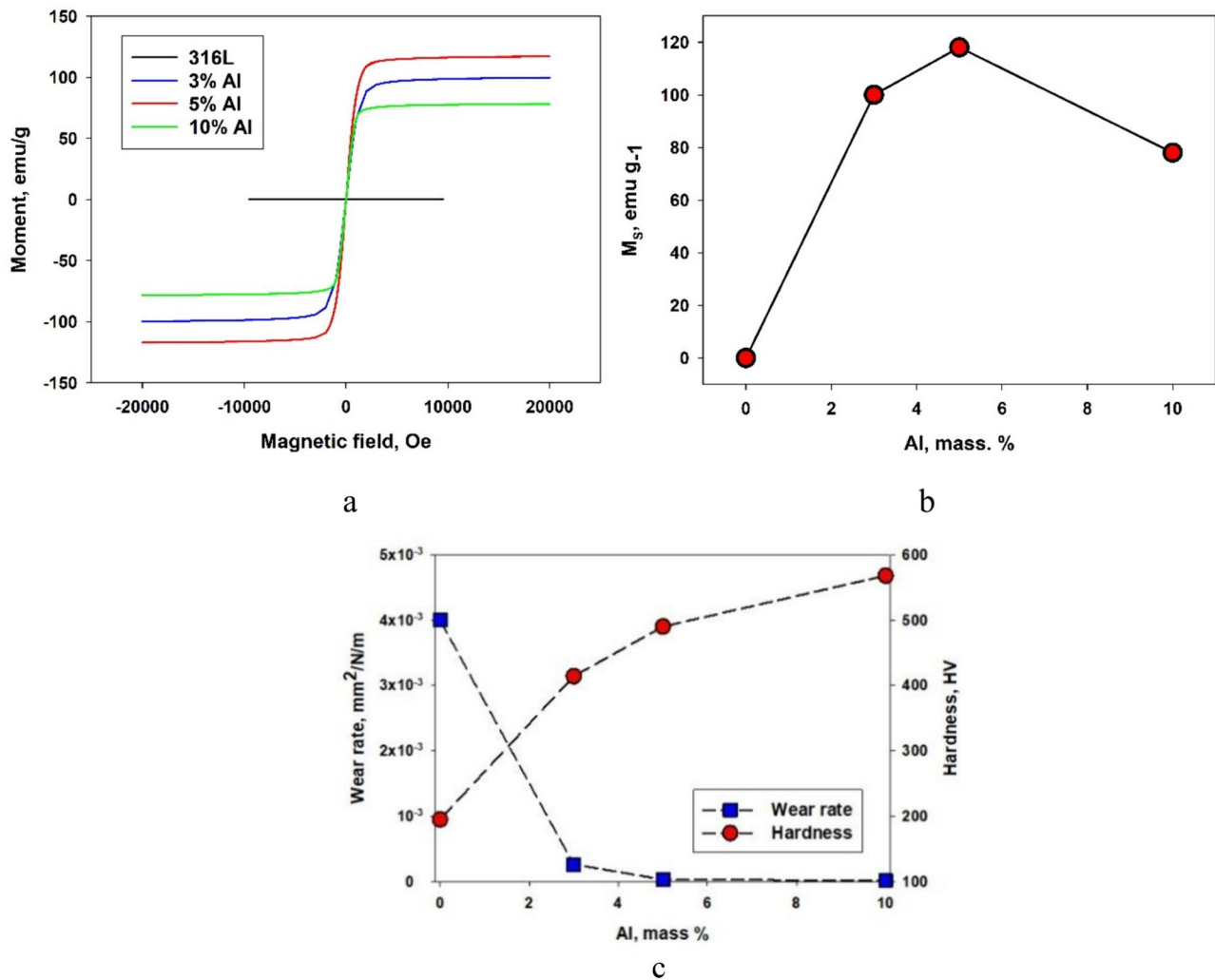


Fig. 2 The effect of Al content on properties of the gradient materials: **a** magnetization curves; **b** the respective values of M_s ; **c** the dependence of wear rate on Al content

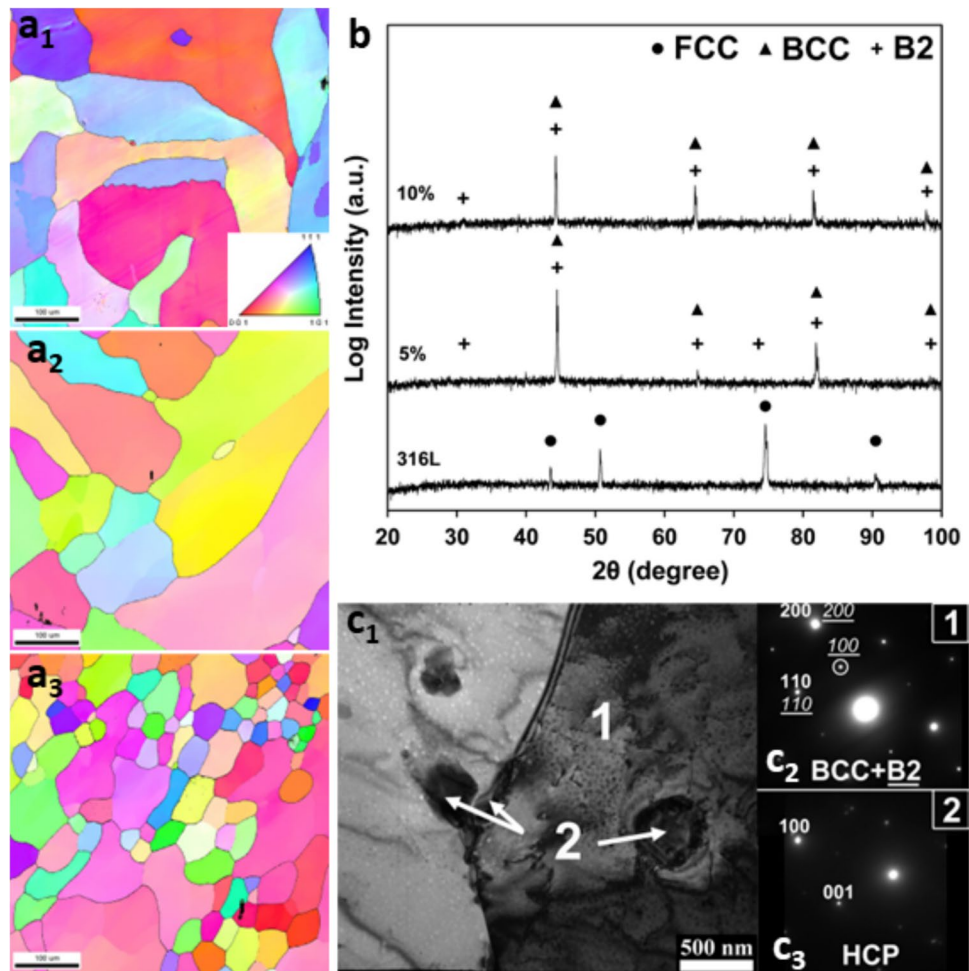
saturated magnetizations (M_s) values were of 100, 118, and 78 emu g⁻¹ for the samples with the Al content of 3, 5, and 10 mass.%, respectively (Fig. 2b). It is noteworthy the maximum of M_s was observed at the Al content of 5%. The wear resistance shows a different trend (Fig. 2c). Increasing the Al content from 0 to 5–10% leads to a decrease in the wear rate from $\sim 6 \times 10^{-4}$ to $\sim 1.5 - 3.0 \times 10^{-5}$ mm²/N/m. It should be noted that the wear was inversely proportional to variations in hardness, which aligns with the well-known relationship [20, 21].

Such changes in properties can be associated with variations in the phase composition. The XRD results clearly demonstrate the pronounced effect of the variations of the chemistry in the mixture of Al and 316L steel (Fig. 3b). The “pure” 316L steel has a single FCC phase structure with the lattice parameters of 0.360 nm. However, even slight additions of Al (5 and 10%) to the steel resulted in the formation

of a BCC-based structure. Moreover, splitting of BCC peaks and appearance of the superlattice reflections can be associated with the formation of a dual-phase BCC + B2 structure. Both phases have similar lattice parameters in the range of 0.288–0.289 nm.

Furthermore, the microstructure of the alloys was examined using the EBSD method (Fig. 3a). It should be noted that the phase maps (not shown here) confirmed XRD data and revealed the FCC structure of the “pure” steel and BCC structure of 5 wt.% and 10 wt.% Al samples. The 316L sample presented a coarse-grained microstructure with irregularly shaped grains measuring approximately ~ 280 μ m (Fig. 3a1). A similar structure with somewhat finer grains (~ 220 μ m) was found in the sample with 5 wt.% Al (Fig. 2a2). Significantly finer (~ 90 μ m) grains with polygonal shape were observed in the 10 wt.% Al sample (Fig. 3a2). Note that local chemical analysis by energy-dispersive

Fig. 3 Structure of the obtained gradient materials; **a** EBSD IPF maps: a_1 316L steel; a_2 5% Al; a_3 10% Al; **b**—XRD patterns; **c** TEM investigations of the 5% Al specimens: c_1 TEM bright-field image; c_2 and c_3 selected area electron diffraction patterns from structural constituents identified with arrows in Fig. 3c1



spectrometry (data not shown) have revealed good chemical homogeneity of 5 wt.% and 10% Al samples.

In addition, TEM studies were conducted of the 5 wt.% Al sample (Fig. 3c). The alloy consisted predominantly of the mixture of the bcc and B2 phases (shown with #1 in Fig. 2c1), with fine cuboidal B2 particles (~60–80 nm) dispersed in the bcc matrix. In addition, some coarser (#2 in Fig. 3c1) particles with hexagonal structure were found mostly adjacent to the BCC grains. Local chemical analysis (results are not shown) suggested that these particles are most likely the Fe_5Si_3 silicide which is typical for AM materials [22].

To provide a rationalization for the obtained findings, a CALPHAD analysis (i.e., calculation of equilibrium phase composition) was conducted to assess the anticipated effect of Al on the phase composition of 316L steel (Fig. 4). While some amount of the BCC phase is expected to form during solidification, the steel is characterized by a stable austenitic (FCC) phase structure with small fraction of secondary phases (carbides and sigma) (Fig. 3a). Addition of relatively small amount of Al (5 mass.%) results in drastic changes in anticipated structure (Fig. 3b). A fully ferritic

(BCC) structure is anticipated with no signs of the FCC phase. In addition to carbides and sigma phases, significant amount of FeAl-type B2 phase is anticipated in precipitates at $T < 1000^\circ\text{C}$. The experimental structure of the alloys (Fig. 3) agree reasonably with the predictions; note also that the BCC + B2 structure is found in Al-doped ferritic steels [23, 24], as well as in some high entropy alloys [25].

The variations in properties with different Al content (Fig. 2) are evidently linked with the changes in the structure (Fig. 3). In terms of magnetic properties, it is well known that austenitic (FCC) steels like 316L are paramagnetic, while the ferritic (BCC) steels exhibit ferromagnetic behavior below the Curie temperatures. Thus, the changes in the magnetic properties of the gradient material are associated with the change in the crystal structure, similarly to many reported magnetic high entropy alloys [17]. In addition, the precipitation of the B2 particles can also have an impact on magnetic properties since inter-phase boundaries can also be pinning sites for the magnetic domains [17]. The variations in the fraction/size of B2 particles can be the reason for the formation of different magnetic properties with 5 and 10 mass.% of Al.

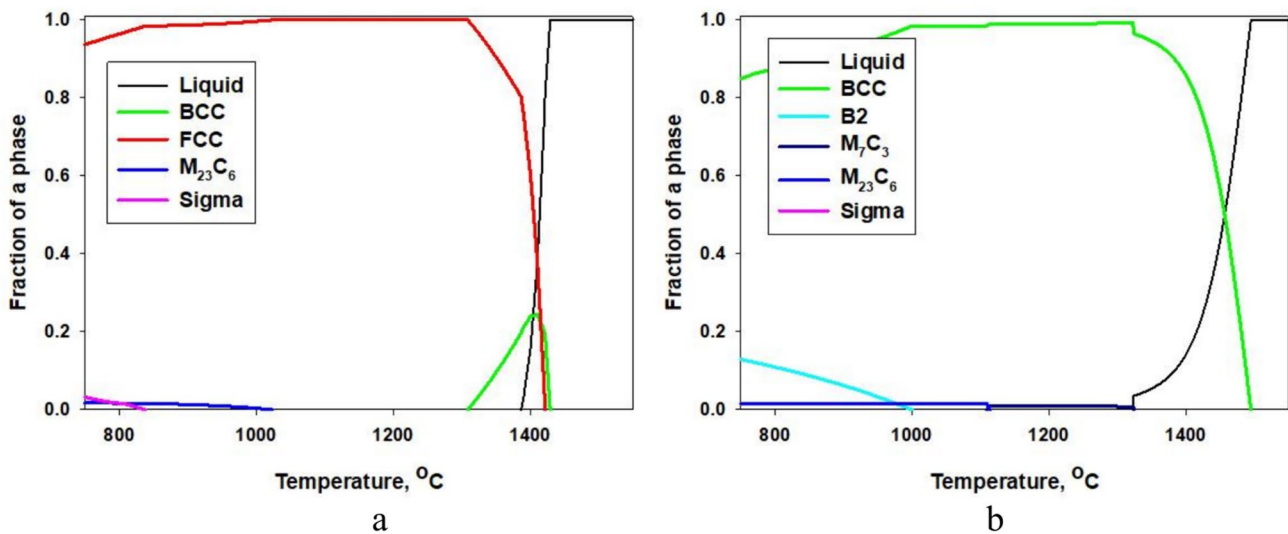


Fig. 4 The calculated equilibrium temperature dependencies of the phase composition (“phase diagrams”) of the: **a** 316L steel, **b** 316L steel with 5% Al

In addition to the B2 particles side, the changes in the chemical composition of the material itself can have strong impact on the mechanical properties [26–28].

In terms of wear resistance, the observed changes can also be explained in relation to the phase structure. Austenitic steels usually have poor wear resistance due to their mechanical “softness” [29]. However, the formation of intrinsically harder BCC matrix with numerous nanoscale B2 precipitates which act as effective strengthening agents [23] enhances the hardness and thus the wear resistance of the gradient material produced.

To sum up, in the present study, we have demonstrated the capacity of DED to produce gradient materials with adjustable magnetic and wear properties by addition of Al to 316L steel (an example is shown in Fig. 5, where the Al content in the transition layer gradually increases from 0 to 10%). Both “starting” materials are non-magnetic and mechanically soft, but addition of 5–10 wt.% of Al to steel leads to the formation of a material with ferromagnetic behavior and relatively high wear resistance. This finding can open new routes for efficient production of multifunctional gradient materials for various applications. For example, one of the possible applications is associated with the creation of complex-shaped shielding from (electro)magnetic fields with spatially variable magnetic characteristics [30–33]. The use of cheap steel and Al for creation of such shielding may be attractive from economical point of view also. However, further studies are required to understand in more details the physical nature of the properties variation with composition and structure. In addition, the other ways of adjusting the properties, i.e., annealing treatment, might be explored.



Fig. 5 The appearance of the as-printed gradient material

4 Conclusions

In this work, we have demonstrated the capability of the DED technique to fabricate gradient materials from a mixture of 316L stainless steel and Al. It has been revealed that even a relatively small addition of Al (5–10 wt.%) can:

- Change the structure from fully FCC to dual-phase BCC + B2;
- Turn paramagnetic steel into the ferromagnetic material with saturation magnetization of $\sim 118 \text{ emu g}^{-1}$;

- Enhance the wear resistance from $\sim 6 \times 10^{-4}$ to $\sim 1.5 - 3.0 \times 10^{-5} \text{ mm}^2/\text{N/m}$.

The observed variations in the properties of the gradient materials can allow efficient and cost-effective fabrication of the electromagnetic shielding for different electronic applications.

Acknowledgements This research was funded by the Ministry of Science and Higher Education of the Russian Federation, project No. 20180148 “Soft magnetic high entropy alloys”, within the program “Priority-2030”.

Data availability The data that support the findings of this study will be available from the corresponding author upon reasonable request.

Declarations

Conflict of interest On behalf of all the authors, the corresponding author states that there is no conflict of interest.

References

- ISO/ASTM 52900:2021 - Additive manufacturing — General principles — Fundamentals and vocabulary. <https://www.iso.org/standard/74514.html>. Accessed 9 Jun 2023
- Herzog D, Seyda V, Wycisk E, Emmelmann C (2016) Additive manufacturing of metals. *Acta Mater* 117:371–392. <https://doi.org/10.1016/j.actamat.2016.07.019>
- Altıparmak SC, Xiao B (2021) A market assessment of additive manufacturing potential for the aerospace industry. *J Manuf Process* 68:728–738. <https://doi.org/10.1016/j.jmapro.2021.05.072>
- Vignesh M, Ranjith Kumar G, Sathishkumar M et al (2021) Development of biomedical implants through additive manufacturing: a review. *J Mater Eng Perform* 30:4735–4744. <https://doi.org/10.1007/S11665-021-05578-7/FIGURES/11>
- Chaudhary V, Mantri SA, Ramanujan RV, Banerjee R (2020) Additive manufacturing of magnetic materials. *Prog Mater Sci* 114:100688. <https://doi.org/10.1016/j.pmatsci.2020.100688>
- Vincent M, Frédéric G, Denis N, et al (2021) Additive manufacturing for soft magnetic materials. *Dig InterMag Conf 2021-April*. <https://doi.org/10.1109/INTERMAG42984.2021.9579804>
- Baufeld B, Van der Biest O, Gault R (2010) Additive manufacturing of Ti-6Al-4V components by shaped metal deposition: microstructure and mechanical properties. *Mater Des* 31:S106–S111. <https://doi.org/10.1016/j.matdes.2009.11.032>
- Ding Y, Muñoz-Lerma JA, Trask M et al (2016) Microstructure and mechanical property considerations in additive manufacturing of aluminum alloys. *MRS Bull* 41:745–751. <https://doi.org/10.1557/MRS.2016.214/FIGURES/5>
- Haftlang F, Kim ES, Kim HS (2022) Crystallographic-orientation-dependent magnetic properties of Fe-Ni permalloy in-situ alloyed using additive manufacturing. *J Mater Process Technol* 309:117733. <https://doi.org/10.1016/j.jmatprotec.2022.117733>
- Kustas AB, Susan DF, Johnson KL et al (2018) Characterization of the Fe-Co-1.5V soft ferromagnetic alloy processed by laser engineered net shaping (LENS). *Addit Manuf* 21:41–52. <https://doi.org/10.1016/j.addma.2018.02.006>
- Gushchina MO, Klimova-Korsmik OG, Turichin GA (2022) Direct laser deposition of Cu-Mo functionally graded layers for dissimilar joining titanium alloys and steels. *Mater Lett* 307:131042. <https://doi.org/10.1016/j.matlet.2021.131042>
- Makarenko KI, Konev SD, Dubinin ON, Shishkovsky IV (2022) Mechanical characteristics of laser-deposited sandwich structures and quasi-homogeneous alloys of Fe-Cu system. *Mater Des* 224:111313. <https://doi.org/10.1016/j.matdes.2022.111313>
- Dev Singh D, Arjula S, Raji Reddy A (2021) Functionally graded materials manufactured by direct energy deposition: a review. *Mater Today Proc* 47:2450–2456. <https://doi.org/10.1016/j.matpr.2021.04.536>
- Gushchina MO, Kuzminova YO, Dubinin ON et al (2023) Multi-layer composite Ti-6Al-4 V/Cp-Ti alloy produced by laser direct energy deposition. *Int J Adv Manuf Technol* 124:907–918. <https://doi.org/10.1007/S00170-022-10521-8/FIGURES/9>
- Kuzminova YO, Dubinin ON, Gushchina MO et al (2023) The mechanical behavior of the Ti6Al4V/Ti/Ti6Al4V composite produced by directed energy deposition under impact loading. *Materialia* 27:101684. <https://doi.org/10.1016/j.mtl.2023.101684>
- Chaudhary V, Yadav NM, Mantri SA et al (2020) Additive manufacturing of functionally graded Co-Fe and Ni-Fe magnetic materials. *J Alloys Compd* 823:153817. <https://doi.org/10.1016/j.jallcom.2020.153817>
- Borkar T, Chaudhary V, Gwalani B et al (2017) A combinatorial approach for assessing the magnetic properties of high entropy alloys: role of Cr in AlCoCr1-xFeNi. *Adv Eng Mater* 19:1700048. <https://doi.org/10.1002/ADEM.201700048>
- Dubinin ON, Chernodubov DA, Kuzminova YO et al (2022) Gradient soft magnetic materials produced by additive manufacturing from non-magnetic powders. *J Mater Process Technol* 300:117393. <https://doi.org/10.1016/j.jmatprotec.2021.117393>
- Farfan-Cabrera LI (2019) Tribology of electric vehicles: a review of critical components, current state and future improvement trends. *Tribol Int* 138:473–486. <https://doi.org/10.1016/j.triboint.2019.06.029>
- Moore MA (1974) The relationship between the abrasive wear resistance, hardness and microstructure of ferritic materials. *Wear* 28:59–68. [https://doi.org/10.1016/0043-1648\(74\)90101-X](https://doi.org/10.1016/0043-1648(74)90101-X)
- Bressan JD, Daros DP, Sokolowski A et al (2008) Influence of hardness on the wear resistance of 17–4 PH stainless steel evaluated by the pin-on-disc testing. *J Mater Process Technol* 205:353–359. <https://doi.org/10.1016/j.jmatprotec.2007.11.251>
- Wang YM, Voisin T, McKeown JT et al (2017) Additively manufactured hierarchical stainless steels with high strength and ductility. *Nat Mater* 17(17):63–71. <https://doi.org/10.1038/nmat5021>
- Stallybrass C, Schneider A, Sauthoff G (2005) The strengthening effect of (Ni, Fe)Al precipitates on the mechanical properties at high temperatures of ferritic Fe-Al-Ni-Cr alloys. *Intermetallics*. Elsevier, Amsterdam, pp 1263–1268
- Wang Z, Wang Q, Niu B et al (2021) Coherent precipitation and stability of cuboidal B2 nanoparticles in a ferritic Fe-Cr-Ni-Al superalloy. *Mater Res Lett* 9:458–466. https://doi.org/10.1080/21663831.2021.1973130/SUPPL_FILE/TMRL_A_1973130_SM2809.DOCX
- Stepanov ND, Shaysultanov DG, Chernichenko RS et al (2019) Effect of Al on structure and mechanical properties of Fe-Mn-Cr-Ni-Al non-equiatom high entropy alloys with high Fe content. *J Alloys Compd*. <https://doi.org/10.1016/j.jallcom.2018.08.093>
- Li P, Wang A, Liu CT (2017) Composition dependence of structure, physical and mechanical properties of FeCoNi(MnAl)_x high entropy alloys. *Intermetallics* 87:21–26. <https://doi.org/10.1016/j.intermet.2017.04.007>
- Ma Y, Wang Q, Zhou X et al (2021) A novel soft-magnetic B2-based multiprincipal-element alloy with a uniform distribution of coherent body-centered-cubic nanoprecipitates. *Adv Mater* 33:2006723. <https://doi.org/10.1002/adma.202006723>

28. Wang Z, Yuan J, Wang Q et al (2024) Developing novel high-temperature soft-magnetic B2-based multi-principal-element alloys with coherent body-centered-cubic nanoprecipitates. *Acta Mater* 266:119686. <https://doi.org/10.1016/J.ACTAMAT.2024.119686>
29. Hegelmann E, Hengst P, Hollmann P et al (2019) Improvement of wear and corrosion resistance of austenitic stainless steel by combined treatment using electron beam cladding and subsequent gas nitrocarburizing. *Adv Eng Mater* 21:1900365. <https://doi.org/10.1002/ADEM.201900365>
30. Okazaki Y, Ueno K (1992) Magnetic shielding by soft magnetic materials in alternating magnetic field. *J Magn Magn Mater* 112:192–194. [https://doi.org/10.1016/0304-8853\(92\)91150-R](https://doi.org/10.1016/0304-8853(92)91150-R)
31. Haneczok G, Wroczynski R, Kwapuliński P et al (2009) Electro/magnetic shielding effectiveness of soft magnetic Fe80Nb6B14 amorphous alloy. *J Mater Process Technol* 209:2356–2360. <https://doi.org/10.1016/J.JMATPROTEC.2008.05.026>
32. Li B, Fu W, Xu H et al (2020) Additively manufactured Ni-15Fe-5Mo Permalloy via selective laser melting and subsequent annealing for magnetic-shielding structures: process, micro-structural and soft-magnetic characteristics. *J Magn Magn Mater* 494:165754. <https://doi.org/10.1016/J.JMMM.2019.165754>
33. Mohamed AEMA, Zou J, Sheridan RS et al (2020) Magnetic shielding promotion via the control of magnetic anisotropy and thermal Post processing in laser powder bed fusion processed NiFeMo-based soft magnet. *Addit Manuf* 32:101079. <https://doi.org/10.1016/J.ADDMA.2020.101079>

Publisher's Note Springer Nature remains neutral with regard to jurisdictional claims in published maps and institutional affiliations.

Springer Nature or its licensor (e.g. a society or other partner) holds exclusive rights to this article under a publishing agreement with the author(s) or other rightsholder(s); author self-archiving of the accepted manuscript version of this article is solely governed by the terms of such publishing agreement and applicable law.